# Multiscale Analytical Sensitivity Analysis for Composite Materials

**Jacob Fish and Amine Ghouali**
*Departments of Civil, Mechanical and Aerospace Engineering*
*Rensselaer Polytechnic Institute, Troy, New York 12180, USA.*

**Abstract**

We describe a methodology aimed at determining the sensitivity of the global structural behavior, such deformation or vibration modes with respect to the local characteristics such as material constants of micro-constituents. An analytical gradient computation, which involves the direct differentiation of the multiple scale strong forms with respect to the design parameters is developed. Comparison of the Multiple Scale Sensitivity Analysis (MASA) to the central finite difference (CFD) approximation in terms of accuracy and computation efficiency is carried out. We demonstrate the robustness of the MASA approach compared to the CFD approximation, which has been found to be highly sensitive to the choice of the step size, whose optimal value is problem dependent.

## 1. Introduction

Composite materials play an important role in many fields of modern engineering due to low weight/stiffness ratio that makes their application in high performance structures very desirable [1]. One of the greatest challenges facing the composites designers today is in selecting nearly optimal material architectures including micro-geometry and properties of micro-phases [2]. The ability to perform micro-structural optimization depends on the accuracy and computational efficiency of the design sensitivity analysis [3], [4].

Design sensitivity analysis deals with a gradient computation of an objective function and constraints with respect to geometrical and/or material characteristics [5], [6]. Typically, this computation is performed numerically by means of the central finite difference approximation [7], [8]. In this case the discrete thermo-mechanical problem is solved for at least two different, but nearby, values of each design parameter. To ensure robustness a convergence study involving several discrete analyses for each design parameter is often performed to determine the required step size. When the total number of independent design parameters becomes large this approach may consume more than two thirds of the total computational cost of the optimization process [9]. Furthermore, the accuracy of the approximations obtained by the finite difference method may not be adequate, in particular for nonlinear history dependent problems [10], [11], or when the actual sensitivities are of the order of numerical errors [12]. One of the alternatives, is the *semi-analytical method* [13], [14], which is based on the differentiation of the discrete equations with respect to the design parameters and subsequent finite difference approximation. Finally, the *analytical approach* is finite difference-free, despite its high complexity [11], [15], [16], [17], [18].

The present manuscript is largely motivated by a desire to develop a Multiscale Analytical Sensitivity Analysis (MASA), with the intent of calibrating microscale material properties to observable experimental data. Multiscale calibration consists of solving the inverse problem leading to a unique and reliable determination of constitutive laws at multiple scales. The goal of the multiple scale sensitivity analysis is to determine the sensitivity of the global behavior, such deformation or vibration modes with respect to material constants of micro-phases and vise versa.

The manuscript is organized as follows. In section 2, the multiple scale inverse problem is formulated as a minimization of the difference between the measured and computed data of interest. The analytical gradient computation involves a direct differentiation of the multiple scale strong forms with respect to the design parameters. In section 3, the mathematical homogenization theory is given for the metal matrix composites. The use of a double scale asymptotic expansion introduces two uncoupled (micro- and macro-) direct problems. The weak form and the corresponding finite element discretization of the two problems are then stated. In section 4, the Multiscale Analytical Sensitivity Analysis (MASA) is developed using the double scale asymptotic expansion for the sensitivities. In section 5, the finite element discretization and the nonlinear solution of the discrete macro and micro sensitivity equations is presented. Finally, two examples are used to validate the present formulation: the first for a linear isotropic elastic composite, and the latter for the linear isotropic elastic reinforcement embedded in the elastoplastic matrix. Comparison of the MASA approach to the CFD approximation in terms of accuracy and computation efficiency completes the manuscript. We show that the CFD approximation is highly sensitive to the choice of the step size, whose optimal value is problem dependent.

## 2. Indirect Calibration of Multiscale Constitutive Equations

In this section, we focus on the mathematical formulation of the problem associated with the optimal design of material microstructure. The ultimate goal is to control the geometrical and material characteristics of the micro-constituents by means of solving the inverse problem which calibrates the computed data to the available experimental measurements at multiple scales. The experimental data on the microscale can be obtained, for example, using the Moire Interferometry technique [19], [20], which produces contour maps of the displacement and strain fields. For an alternative technique based on the topological micro-structural optimization we refer to [24].

### 2.1. *Multiscale Inverse Problem.*

We consider a periodic composite structure defined by two scales: the macroscale with a position vector $x(x_1,x_2,x_3)$ defined on the domain $\Omega$ and the microscale with a position vector $y(y_1,y_2,y_3)$ defined on the Representative Volume Element (RVE) domain $\Theta$ as shown in Fig. 1. The position vectors on the micro- and macro- scales are related by the small parameter $I$ $\left(y = x/\in\right)$, which is the ratio of the two scale characteristic lengths. The micro-constituents are assumed to possess homogeneous properties and to satisfy equilibrium, constitutive, kinematics and compatibility equations, as well as jump conditions at the interface between the micro-constituents.

The two-scale inverse problem consists of minimizing the error between the measured and computed data. Assuming that the experimental data, such as displacements $\hat{u}$ and strain field are available, the minimization problem can be stated as follows:

$$\begin{cases} \textit{Find the control field } P(p_a) \textit{ such that} \\ \underset{P\in\,\Pi}{Min}\left( f(P) \;=\; v_1 \int\limits_{\Omega^*} \left\| u-\hat{u} \right\|^2 d\Omega \;+\; v_2 \int\limits_{\Omega^*} \left[ \frac{1}{\left|\Theta^*\right|} \int\limits_{\Theta^*} \left\| e(u)-\hat{e} \right\|^2 d\Theta \right] d\Omega \right) \end{cases} \tag{1}$$

where $\Pi$ is the space of admissible design variables; $\Theta^*$ and $\Omega^*$ are the portions of the micro and macro domains, respectively, where the experimental data is available; $P(p_a)$ is the set of parameters defining constitutive laws on the microscale, such as Young modulus, Poisson ratio, hardening modulus and yield stress of micro-phases; $\varpi_1$ and $\varpi_2$ are weighting parameters; $u$ is the computed displacement field on $\Omega^*$; and $e(u)$ is the computed local strain field on $\Theta^*$.

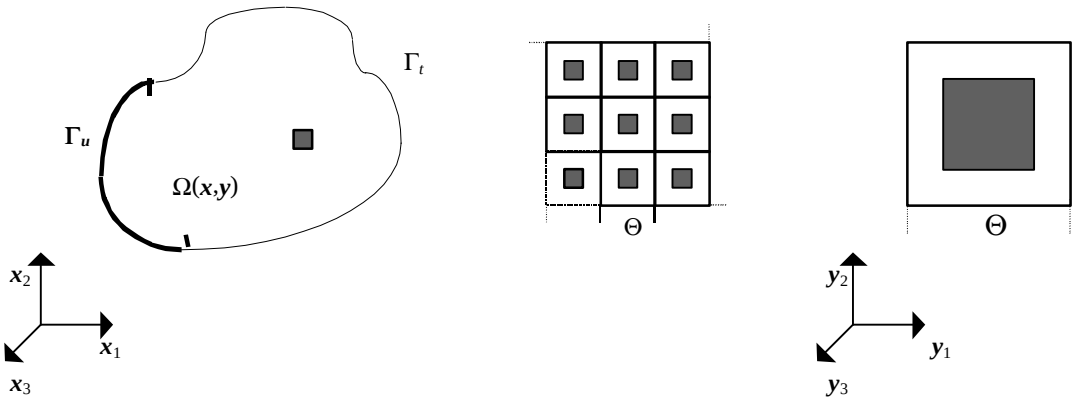

Fig. 1. (a) The macro domain $\Omega$, and (b) the Representative Volume Element domain $\Theta$.

Various sensitivity analysis approaches required for solving the constrained minimization problem (1) are briefly summarized in the next section.

### 2.2. Design sensitivity analysis

One approach by which the gradient computation can be obtained is the central finite difference (CFD) approximation:

$$\frac{df}{dp_a} \cong \frac{\Delta f}{\Delta p_a} \equiv \frac{f(p_a + d\,p_a) - f(p_a - d\,p_a)}{2d\,p_a} \tag{2}$$

where $d\,p_a$ denotes a small step size.

Typically, the gradient computation using the finite difference approximation requires several solutions of the problem for each finite difference increment. In order to ensure sufficiently accurate sensitivities a convergence study is often performed [21], which involves several analyses for each design parameter. For large scale problems, the computational cost might be prohibitive as it may entail more than two thirds of the optimization process [12]. Furthermore, the accuracy of the approximations obtained by the finite difference approximation may not be adequate in particular for nonlinear history dependent problems [10], [11] or when the actual sensitivities are of the order of numerical errors [16]. An alternative, which is adopted in the present manuscript, is based on the analytical differentiation [3], [18]. In the present context it involves a direct differentiation of the multiple scale strong forms with respect to the design parameters.

## 3. Review of the mathematical homogenization theory

### 3.1. *Macro-Scale Direct Problem*

Due to the periodic nature of the microstructure any response function $g^{\epsilon}(x) = g(x, y(x))$, such as displacements $u_i^{\epsilon}$, stresses $s_{ij}^{\epsilon}$, and strains $e_{ij}(u^{\epsilon})$, defined on the composite domain $\Omega$ *(x, y)*, are also *y*-periodic. The boundary value boundary problem is governed by the following equations:

$$s_{ij,x_j}^{\epsilon} + b_i(x) = 0 \qquad \text{in} \qquad \Omega(x, y) \tag{3}$$

$$\dot{s}_{ij}^{\epsilon} = L_{ijkh}\, \dot{e}_{kh}(u^{\epsilon}) \qquad \text{in} \qquad \Omega(x, y) \tag{4}$$

$$\dot{e}_{ij}(u^{\epsilon}) = \dot{u}_{(i,x_j)}^{\epsilon} \qquad \text{in} \qquad \Omega(x, y) \tag{5}$$

$$u_i^{\epsilon} = \bar{u}_i(x) \qquad in \qquad \Gamma_t \tag{6}$$

$$s_{ij}^{\epsilon} n_j = \bar{t}_i(x) \qquad \text{in} \qquad \Gamma_u \tag{7}$$

where the superimposed dot represents the material time derivative; $\dot{u}_i^{\epsilon}$ and $\dot{e}_{ij}^{\epsilon}$ are the velocity vector and the rate of deformation tensor, respectively; the subscript pair with parentheses denotes the symmetric gradient defined as $\dot{u}_{(i,x_j)}^{\epsilon} = \left(\dot{u}_{i,x_j}^{\epsilon} + \dot{u}_{j,x_i}^{\epsilon}\right)/2$; $b_i(x)$, $\bar{u}_i(x)$ and $\bar{t}_i(x)$ are the body forces on $\Omega$, the prescribed displacements on $\Gamma_u$ and the prescribed boundary tractions on $\Gamma_t$, respectively; $L_{ijkh}$ is the instantaneous constitutive tensor and $n_j$ is the normal to $\Gamma_t$. Attention is restricted to small deformation theory.

The multiple scale analysis of the strong form (3)-(7) is obtained by approximating the velocity field as:

$$\dot{u}_i^{\epsilon}(x) = \dot{u}(x, y) = \dot{u}_i^{0}(x, y) + \epsilon\, \dot{u}_i^{1}(x, y) + .... \tag{8}$$

Using the chain rule, the macroscopic spatial derivative of the velocity field (8) is given by:

$$\dot{u}_{i,x_i}^{\epsilon}(x) = \frac{\partial \dot{u}_i^{\epsilon}(x)}{\partial x_j} = \left(\frac{\partial}{\partial x_j} + \epsilon^{-1}\frac{\partial}{\partial y_j}\right)\dot{u}_i(x, y) = \dot{u}_{i,x_j}(x, y) + \epsilon^{-1}\dot{u}_{i,y_j}(x, y) \tag{9}$$

From (7) and (8), we obtain the following expansion of the rate of strain field:

$$\dot{e}_{ij}(u^{\epsilon}(x)) \equiv e_{ij}(\dot{u}(x, y)) \approx \epsilon^{-1} e_{ij}^{-1}(\dot{u}(x, y)) + e_{ij}^{0}(\dot{u}(x, y)) + \epsilon\, e_{ij}^{1}(\dot{u}(x, y)) + ... \tag{10}$$

where

$$e_{ij}^{-1}(\mathfrak{u}(x,y)) = \mathfrak{u}_{(i,y_j)}^{0}(x,y) \tag{11}$$

$$e_{ij}^{0}(\mathfrak{u}(x,y)) = \mathfrak{u}_{(i,x_j)}^{0}(x,y) + \mathfrak{u}_{(i,y_j)}^{1}(x,y) \tag{12}$$

$$e_{ij}^{1}(\mathfrak{u}(x,y)) = \mathfrak{u}_{(i,x_j)}^{1}(x,y) + \mathfrak{u}_{(i,y_j)}^{2}(x,y) \tag{13}$$

The expansion of the stress rate is obtained by substituting the strain rate approximation (10) into the constitutive equation (3) which yields:

$$\mathfrak{s}_{ij}^{\in}(x) \equiv \mathfrak{s}_{ij}(x,y) \approx \in^{-1} \mathfrak{s}_{ij}^{-1}(x,y) + \mathfrak{s}_{ij}^{0}(x,y) + \in \mathfrak{s}_{ij}^{1}(x,y) + \ldots \tag{14.$a$}$$

where

$$\mathfrak{s}_{ij}^{s} = L_{ijkh}\, e_{kh}^{s}(\mathfrak{u}(x,y)), \qquad s = -1,0,1,\ldots \tag{14.$b$}$$

Similarly, the expansion for the stress field is given by:

$$s_{ij}^{\in}(x) \equiv s_{ij}(x,y) \approx \in^{-1} s_{ij}^{-1}(x,y) + s_{ij}^{0}(x,y) + \in s_{ij}^{1}(x,y) + \ldots \tag{15}$$

Inserting the stress asymptotic expansion (14.$a$) into equilibrium equations (3) and making use of the chain rule yields various order equilibrium equations:

$$\mathrm{O}(\hat{I}^{-2}): \quad s_{ij,y_j}^{-1} = 0 \tag{16}$$

$$\mathrm{O}(\hat{I}^{-1}): \quad s_{ij,x_j}^{-1} + s_{ij,y_j}^{-0} = 0 \tag{17}$$

$$\mathrm{O}(\hat{I}^{0}): \quad s_{ij,x_j}^{0} + s_{ij,y_j}^{1} + b_i = 0 \tag{18}$$

$$\mathrm{O}(\hat{I}^{s}): \quad s_{ij,x_j}^{s} + s_{ij,y_j}^{s+1} = 0, \quad s = 1,2,\ldots \tag{19}$$

To solve for the $\mathrm{O}(\hat{I}^{-2})$ equilibrium equation we pre-multiply the rate form of (16) by $\mathfrak{u}_i^0$ and integrate it over RVE domain, $\Theta$, which yields

$$\int_{\Theta} \mathfrak{u}_i^0\, \mathfrak{s}_{ij,y_j}^{-1}\, d\Theta = 0 \tag{20}$$

and subsequent integration by parts results in

$$\int_{\Gamma_\Theta} \mathfrak{u}_i^0\, \mathfrak{s}_{ij}^{-1} n_j\, d\Gamma_\Theta - \int_{\Theta} \mathfrak{u}_{(i,y_j)}^{0}\, L_{ijkh}\, \mathfrak{u}_{(h,y_k)}^{0}\, d\Theta = 0 \tag{21}$$

where the first term in the above equation vanishes due to periodicity of the boundary conditions on $\Gamma_\Theta$. Assuming that the instantaneous stiffness tensor $L_{ijkh}(y)$ is positive definite the unique solution of the equilibrium equation (21) is

$$\mathfrak{u}^0_{(i,y_j)} = 0 \quad \Rightarrow \quad \mathfrak{u}^0_i = \mathfrak{u}^0_i(x) \tag{22}$$

The strong form of the $O(\hat{I}^{-1})$ equilibrium follows from (15) and the rate form of (17) which yields

$$\left( L_{ijkh} \left( \mathfrak{u}^0_{(k,x_h)} + \mathfrak{u}^1_{(k,y_h)} \right) \right)_{,y_j} = 0 \tag{23}$$

To solve for (23) up to a constant we introduce the following separation of variables

$$\mathfrak{u}^1_i(x, y) = \mathfrak{R}^{mn}_i(y)\, \mathfrak{u}^0_{(m,x_n)}(x) \tag{24}$$

in which $\mathfrak{R}^{mn}_i$ represents the instantaneous *y*-periodic function with symmetry with respect to indexes *m* and *n*.

We further denote

$$\Psi^{mn}_{ij}(y) = \mathfrak{R}^{mn}_{(i,y_j)}(y) \tag{25}$$

and the equilibrium equation (23) can be expressed as

$$\left( L_{ijkh} \left( I_{khmn} + \Psi^{kh}_{mn}(y) \right) \mathfrak{u}^0_{(m,x_n)}(x) \right)_{,y_j} \tag{26}$$

where

$$I_{khmn} = \frac{1}{2}(d_{km}d_{hn} + d_{kn}d_{hm}) \tag{27}$$

and $d_{km}$ is the Kronecker delta. For an arbitrary macroscopic velocity field $\mathfrak{u}^0_i$ equation (26) yields

$$\left( L_{ijkh} \left( I_{khmn} + \Psi^{kh}_{mn}(y) \right) \right)_{,y_j} = 0 \tag{28}$$

To solve for the $O(\hat{I}^{0})$ equilibrium equation we integrate the rate form of (18) over RVE domain which yields

$$\int_\Theta \left( L_{ijkh}(y)\, \mathfrak{u}^1_{(k,x_h)} \right)_{,y_j} d\Theta + \int_\Theta L_{ijkh}(y) \left( \mathfrak{u}^1_{(k,y_h)} + \mathfrak{u}^0_{(k,x_h)} \right)_{,x_j} d\Theta + \int_\Theta \mathfrak{b}_i\, d\Theta = 0 \tag{29}$$

where the first term vanishes due to the periodicity resulting in

$$\left( \left[ \int_{\Theta} L_{ijkh}(y) \left( I_{khmn} + \Psi_{kh}^{mn} \right) d\Theta \right] \varepsilon^{0}_{(m,x_n)} \right)_{,x_j} + |\Theta| b_i = 0 \tag{30}$$

where $|\Theta|$ is the volume of the RVE. The rate of the local stress field,

$$\sigma_{ij} = L_{ijkh}(y) \left( I_{khmn} + \Psi_{kh}^{mn} \right) \varepsilon_{mn}(u), \tag{31}$$

the macroscopic strain rate field, $\varepsilon_{mn}(u) = \varepsilon^{0}_{(m,x_n)}(x)$, and the overall stress field

$$\bar{\sigma}_{ij} = \frac{1}{|\Theta|} \int_{\Theta} \sigma_{ij} \, d\Theta = \frac{1}{|\Theta|} \int_{\Theta} L_{ijkh}(y) \left( I_{khmn} + \Psi_{kh}^{mn} \right) d\Theta \; \bar{\varepsilon}_{mn}(u) \tag{32}$$

are defined in the usual manner [1], [22], [23].

From (29) the macroscopic equilibrium equation can be cast into the familiar form

$$\bar{\sigma}_{ij,\,x_j} + b_i = 0 \tag{33}$$

Further denoting the homogenized stiffness tensor components as

$$\bar{L}_{ijkh} = \frac{1}{|\Theta|} \int_{\Theta} L_{ijmn}(y) \left( I_{khmn} + \Psi_{kh}^{mn} \right) d\Theta \tag{34}$$

the strong form of the macro-scale direct global problem (3)-(7) can be re-written as follows:

$$\begin{cases} \bar{\sigma}_{ij,\,x_j} = -b_i & in \quad \Omega \\ \bar{\sigma}_{ij} = \bar{L}_{ijkh}(\Re)\, \bar{\varepsilon}_{kh}(u) & in \quad \Omega \\ \bar{\varepsilon}_{ij}(u) = \varepsilon^{0}_{(i,x_j)} & in \quad \Omega \\ u_i = \bar{u}_i & on \quad \Gamma_u \\ \bar{\sigma}_{ij} n_j = \bar{t}_i & on \quad \Gamma_t \end{cases} \tag{35}$$

### 3.2. *Micro-Scale Direct Problem*

The solution of the boundary value problem (35) is a function of the characteristic function $\Re_i^{mn}$. Further expressing the stress concentration factors on $\Theta$ as

$$s_{ij}^{kh} = L_{ijmn}(y) \left( I_{khmn} + \Psi_{mn}^{kh} \right), \tag{36}$$

the characteristic functions $\aleph_i^{mn}$ and $s_{ij}^{kh}$ are the solutions of the following micro-scale direct problem:

$$\begin{cases} \aleph_i^{mn} & is & y-periodic & & \\ s_{ij,y_j}^{kh} & = & 0 & in & \Theta \\ s_{ij}^{kh} & = & L_{ijmn}(y)\,(I_{khmn} + \Psi_{mn}^{kh}) & in & \Theta \\ \left[\left|\aleph_i^{mn}\right|\right] & = & 0 & on & g_\Theta \\ \left[\left|s_{ij}^{kh}\, n_j\right|\right] & = & 0 & on & g_\Theta \\ s_{ij}^{kh}\, n_j & is & y-antiperiodic & & \end{cases} \tag{37}$$

where $\left[\left|\bullet\right|\right]$ denotes the jump operator at the interface between the micro-constituents $g_\Theta$.

The instantaneous strain concentration function $\Im_{kh}^{ij}(y)$ is denoted as

$$\Im_{kh}^{ij}(y) = I_{ijkh} + \Psi_{kh}^{ij}(y) \tag{38}$$

so that the local strain rate field $\dot{\varepsilon}_{ij}(u(x,y))$ is given by:

$$\dot{\varepsilon}_{ij}(u(x,y)) = \Im_{mn}^{ij}(y)\,\dot{\varepsilon}_{mn}(u) \tag{39}$$

### 3.3 The weak and the discrete forms

The weak form of (35) is given as:

$$\begin{cases} find\ \ u_i^0 \in U_{ad}\ such\ that: \\ \\ \displaystyle\int_\Omega \dot{s}_{ij}(u^0)\ \ e_{ij}(j)\,d\Omega = \int_\Omega b_i\ j_i\,d\Omega + \int_{\Gamma_t} \overline{t}_i\ j_i\,d\Gamma\ ; \quad \forall j_i \in U_{ad}^*; \end{cases} \tag{40}$$

where $U_{\text{ad}}$ is the admissible space defined by:

$$U_{ad} = \left\{ u_i \in \left[H^1(\Omega)\right]^3 \ \ / \ \ u_i = \overline{u}_i \ \ on \ \ \Gamma_u \right\} \tag{41}$$

$H^1(\Omega)$ is the Hilbert space and $U_{\text{ad}}^*$ is the vector space defined as:

$$U_{ad}^* = \left\{ u_i \in \left[H^1(\Omega)\right]^3 \ \ / \ \ u_i = 0 \ \ on \ \ \Gamma_u \right\} \tag{42}$$

The system of nonlinear equations arising from the finite element discretization of (40) yields:

$$r_A = f_A^{ext} - f_A^{\text{int}} = 0 \tag{43}$$

where $r_A$ is the residual vector and

$$f_A^{\text{int}}(u_i) = \int_\Omega \sigma_{kh}(u_i)\, B_{khA}^{\Omega}\, d\Omega \;\; ; \qquad f_A^{ext} = \int_\Omega b_j\, N_{jA}^{\Omega}\, d\Omega + \int_{\Gamma_t} \bar{t}_j\, N_{jA}^{\Omega}\, d\Gamma \tag{44}$$

are the components of the internal and external force vectors, respectively; $N_{jA}^{\Omega}$ are the shape functions defined on $\Omega$; $B_{khA}^{\Omega}$ are the corresponding spatial derivatives $\left(B_{jiA}^{\Omega} = N_{(jA,i)}^{\Omega}\right)$.

Let $d_A$ $\left(u_i = N_{iA}^{\Omega}\, d_A\right)$ be the nodal components of the displacement field. The discrete equation (43) is solved using the Newton method such that:

$${}^{(k+1)}d_A = {}^{(k)}d_A + \Delta d_A \tag{45}$$

where the displacement increment, $\Delta d_A$ , for each iteration *(k)*, from is obtained:

$${}^{(k)}K_{AB}\;\Delta d_A \;=\; {}^{(k)}r_A \tag{46}$$

$$K_{AB} = \frac{\partial r_A}{\partial d_B} = \int_\Omega B_{mnA}^{\Omega}\, L_{mnkh}\, B_{khB}^{\Omega}\, d\Omega \tag{47}$$

The instantaneous characteristic function $\Re_i^{rs}$ is a solution of the following micro-scale weak form:

$$\begin{cases} Find \;\; \Re_i^{rs} \in \left[H^1(\Theta)\right]^3 \;\; such\, that \\ \\ \displaystyle\int_\Theta \Re_{i,j}^{rs}\, L_{ijkh}\, j_{k,h}\, d\Theta = -\int_\Theta L_{ijrs}\, j_{i,j}\, d\Theta \;; \quad \forall j_i \in \left[H^1(\Theta)\right]^3 \end{cases} \tag{48}$$

Let $\mathbf{D}_A^{rs}$ $\left(\Re_i^{rs} = N_{iA}^{\Theta}\, \mathbf{D}_A^{rs}\right)$ be the nodal components of the characteristic functions, then the corresponding discrete form of (48) yields:

$$K_{AB}^{\Theta}\, \mathbf{D}_B^{rs} = \left(\int_\Theta B_{mnA}^{\Theta}\, L_{mnkh}(y)\, B_{khB}^{\Theta}\, d\Theta\right) \mathbf{D}_B^{rs} = -\int_\Theta L_{khrs}(y)\, B_{khA}^{\Theta}\, d\Theta \tag{49}$$

where $K_{AB}^{\Theta}$ is the RVE stiffness matrix; $L_{mnkh}(y)$ the instantaneous constitutive tensor of the micro-phases; $N_{iA}^{\Theta}$ the shape functions on $\Theta$ and $B_{khA}^{\Theta}$ the corresponding symmetric spatial derivatives.

The above two scale nonlinear problem is solved incrementally (see [22], [23]). The stress update procedure is outlined below.

### 3.4. *Stress update procedure*

The constitutive relation for the elasto-plastic microstructure at a typical Gauss point $y_r \in \Theta$ is

$$\dot{s}_r = L_r \dot{\varepsilon}_r^e(u) = L_r \left(\dot{\varepsilon}_r(u) - \dot{\varepsilon}_r^p(u)\right) \tag{50}$$

where $L_r$ is the elastic stiffness matrix ; $\dot{\varepsilon}_r^e(u)$ is the elastic part of the microscopic strain rate (39).

Following the associative flow rule, the plastic strain rate $\dot{\varepsilon}_r^p(u)$ is given by:

$$\dot{\varepsilon}_r^p(u) = \dot{\lambda}_r(u)\, \mathrm{N}_r; \qquad \mathrm{N}_r = \frac{\partial \Phi_r(s)}{\partial s_r} \tag{51}$$

where $\lambda(u)$ is a plastic flow parameter; $\Phi_r(s)$ is Von Mises yield function at a Gauss point, given by:

$$\Phi_r(s) = \frac{1}{2} s_r^{\mathrm{T}} P s_r - \frac{1}{3}\hat{s}_r^2 = 0 \tag{52}$$

For Von Mises plasticity, P is defined as:

$$P = \hat{P}^T T \hat{P}; \qquad \hat{P} = \frac{1}{3}\begin{pmatrix} 2 & -1 & -1 & 0 & 0 & 0 \\ -1 & 2 & -1 & 0 & 0 & 0 \\ -1 & -1 & 2 & 0 & 0 & 0 \\ 0 & 0 & 0 & 3 & 0 & 0 \\ 0 & 0 & 0 & 0 & 3 & 0 \\ 0 & 0 & 0 & 0 & 0 & 3 \end{pmatrix} \tag{53}$$

in which T is 6×6 diagonal matrix with 1 in the first three diagonal locations and 2 in the remaining three diagonal entries; $\hat{P}$ is a projection operator satisfying $\hat{P} = \hat{P}\hat{P}$ and $P = \hat{P}P = P\hat{P}$, which transforms a vector to deviatoric space; $\hat{s}_r$ is the yield stress which evolves according to the hardening law as:

$$\dot{\hat{s}}_r = \frac{2}{3}\dot{\lambda}_r(u)\,\mathrm{H}\,\hat{s}_r; \qquad {}^{(k+1)}\hat{s}_r = {}^{(k)}\hat{s}_r + \frac{2}{3}\Delta l_r(u)\,\mathrm{H}\,{}^{(k+1)}\hat{s}_r \tag{54}$$

where the backward Euler integration scheme is exercised; H is a hardening parameter defined as the ratio between effective stress rate and effective plastic strain rate.

Inserting (39) and (51) into (50) yields

$$\dot{s}_r = L_r \left( \Im_r \dot{\varepsilon}_r(u) - \dot{\Gamma}(u) P s_r \right) \tag{55}$$

and applying the backward Euler scheme gives

$${}^{(k+1)}s_r = \left( I + \Delta l_r(u) L_r P \right)^{-1} s_r^{trial} \tag{56}$$

where $s_\rho^{trial}$ is the trial stress given by:

$$s_r^{trial} = {}^{(k)}s_r + L_r \Im_r \Delta\dot{\varepsilon}_r(u) \tag{57}$$

Note that the instantaneous strain concentration factor $\Im_\rho$ is obtained from the solution of (48) which in turn depends on the instantaneous properties at each Gauss point. For simplicity of numerical implementation we assume:

$${}^{(k+1)}\Im_r = {}^{(k)}\Im_r \tag{58}$$

Substituting (56) into the yield function (52) yields the nonlinear equation with unknown plastic parameter increment $\Delta l_r(u)$ at each Gauss point which can be solved using Newton method

$${}^{(k+1)}\Delta l_r(u) = {}^{(k)}\Delta l_r(u) - \left( \frac{\partial \Phi_r}{\partial \Delta l_r} \right)^{-1} \Phi\big|_{{}^{(k)}\Delta l_r} \tag{59}$$

where

$$\frac{\partial \Phi_r}{\partial \Delta l_r} = -s_r^{\mathrm{T}} P \left( \left( L_r P \right)^{-1} + \Delta l_r(u) \mathrm{H} \right)^{-1} s_r - \frac{4}{9} \mathrm{H} \hat{s}_r^2 \tag{60}$$

Once the incremental plastic parameter $\Delta l_r(u)$ is obtained, the local stress field follows from the integration of (56).

## 4. Multiscale Analytical Sensitivity Analysis.

The Multiscale Analytical Sensitivity Analysis is based on the the direct differentiation of the direct problem (3)-(7) and subsequent multiple scale asymptotic analysis. In the present manuscript, only two-scale sensitivity analysis is considered, even though the methodology can be generalized to multiple scales. Attention is restricted to the sensitivities with respect to material constants.

### 4.1. *Macro-Scale Sensitivity Problem*

We assume that traction and displacement boundary conditions as well as the body force are independent of the design variables. The direct differentiation of the strong form (3)-(7) with respect to the design variables $P(p_a)$ yields:

$$\Sigma^{\epsilon}_{ij,x_j} = 0 \qquad in \qquad \Omega(x,y) \tag{61}$$

$$\dot{\Sigma}^{\epsilon}_{ij} = L_{ijkh}\,\dot{e}_{kh}(w^{\epsilon}) + L'_{ijkh}\,\dot{e}_{kh}(u^{\epsilon}) \qquad in \qquad \Omega(x,y) \tag{62}$$

$$\dot{e}_{ij}(w^{\epsilon}) = \dot{w}^{\epsilon}_{(i,x_j)} \qquad in \qquad \Omega(x,y) \tag{63}$$

$$w^{\epsilon}_i = 0 \qquad in \qquad \Gamma_u \tag{64}$$

$$\Sigma^{\epsilon}_{ij} n_j = 0 \qquad in \qquad \Gamma_t \tag{65}$$

where

$$L'_{ijkh} = \frac{\partial L_{ijkh}}{\partial P} \tag{66}$$

is the sensitivity of the constitutive tensor and

$$w^{\epsilon}_i = \frac{\partial u^{\epsilon}_i}{\partial P}, \tag{67}$$

$$\Sigma^{\epsilon}_{ij} = \frac{\partial s^{\epsilon}_{ij}}{\partial P} \tag{68}$$

are the sensitivities of the displacement and the stress fields, respectively; $\dot{w}^{\epsilon}_i$ and $\dot{\Sigma}^{\epsilon}_{ij}$ denote the corresponding time derivatives.

The double scale asymptotic analysis of the sensitivity problem (61)-(65) is carried out by approximating the solution sensitivity $w^{\epsilon}_i(x)$ as follows:

$$w^{\epsilon}_i(x) = w(x,y) = w^0_i(x,y) + \epsilon\, w^1_i(x,y) + \ldots \tag{69}$$

Applying the chain rule to (69) yields the following expansion of the strain rate sensitivity:

$$\dot{e}_{ij}(w^{\epsilon}(x)) \equiv e_{ij}(\dot{w}(x,y)) \approx \epsilon^{-1} e^{-1}_{ij}(\dot{w}(x,y)) + e^0_{ij}(\dot{w}(x,y)) + \epsilon\, e^1_{ij}(\dot{w}(x,y)) + \ldots \tag{70}$$

where

$$e_{ij}^{-1}(\mathbf{w}(x,y)) = \mathbf{w}^{o}_{(i,y_j)}(x,y) \tag{71}$$

$$e_{ij}^{1}(\mathbf{w}(x,y)) = \mathbf{w}^{0}_{(i,x_j)}(x,y) + \mathbf{w}^{1}_{(i,y_j)}(x,y) \tag{72}$$

$$e_{ij}^{1}(\mathbf{w}(x,y)) = \mathbf{w}^{1}_{(i,x_j)}(x,y) + \mathbf{w}^{2}_{(i,y_j)}(x,y) \tag{73}$$

The approximation of the stress rate sensitivity field is obtained by inserting (70) into the constitutive equation (62), which gives

$$\mathbf{S}^{\in}_{ij}(x) \equiv \mathbf{S}_{ij}(x,y) \approx \in^{-1} \mathbf{S}^{-1}_{ij}(x,y) + \mathbf{S}^{0}_{ij}(x,y) + \in \mathbf{S}^{1}_{ij}(x,y) + \ldots \tag{74}$$

where

$$\mathbf{S}^{s}_{ij} = L_{ijkh}(y)\, \mathbf{e}^{s}_{kh}(w(x,y)) + L'_{ijkh}(y)\, \mathbf{e}^{s}_{kh}(u(x,y)) \qquad s = -1,0,1,\ldots \tag{75}$$

The analogous expression for the stress sensitivity is:

$$\Sigma^{\in}_{ij}(x) \equiv \Sigma_{ij}(x,y) \approx \in^{-1} \Sigma^{-1}_{ij}(x,y) + \Sigma^{0}_{ij}(x,y) + \in \Sigma^{1}_{ij}(x,y) + \ldots \tag{76}$$

Inserting the asymptotic expansion (76) into (61) and using the chain rule yields various orders of sensitivity equations:

$$O(\in^{-2}): \quad \Sigma^{-1}_{ij,y_j} = 0 \tag{77}$$

$$O(\in^{-1}): \quad \Sigma^{-1}_{ij,x_j} + \Sigma^{0}_{ij,y_j} = 0 \tag{78}$$

$$O(\in^{0}): \quad \Sigma^{0}_{ij,x_j} + \Sigma^{1}_{ij,y_j} = 0 \tag{79}$$

$$O(\in^{s}): \quad \Sigma^{s}_{ij,x_j} + \Sigma^{s+1}_{ij,y_j} = 0, \qquad s = 1,2,\ldots \tag{80}$$

To solve for the $O(\hat{I}^{-2})$ sensitivity equation we pre-multiply the time derivative of (77) by $\mathbf{w}^{0}_{i}$, integrate it over the $\Theta$ and then perform integration by parts which yields

$$\int_{\Gamma_\Theta} \mathbf{w}^{0}_{i}\, \Sigma^{-1}_{ij}\, n_j \, d\Gamma_\Theta \; - \int_{\Theta} \mathbf{w}^{0}_{(i,y_j)}\, L'_{ijkh}\, \mathbf{e}^{0}_{(h,y_h)}\, d\Theta \; - \int_{\Theta} \mathbf{w}^{0}_{(i,y_j)}\, L_{ijkh}\, \mathbf{w}^{0}_{(h,y_h)}\, d\Theta = 0 \tag{81}$$

where the first and the second term vanish due to the periodicity of the boundary conditions on $\Gamma_\Theta$ and (22), respectively. Assuming that $L'_{ijkh}$ is positive definite yields the unique solution

$$\mathbf{w}^{0}_{(i,y_j)} = 0 \quad \Rightarrow \quad \mathbf{w}^{0}_{i} = \mathbf{w}^{0}_{i}(x) \tag{82}$$

The strong form of the $O(\hat{I}^{-1})$ equation is obtained from (75) and the rate form of (78) which yields

$$\left(L_{ijkh}\ \left(\mathbb{w}^{0}_{(k,x_h)}+\mathbb{w}^{1}_{(k,y_h)}\right)\right)_{,y_j}+\left(L'_{ijkh}\ \left(\mathbb{u}^{0}_{(k,x_h)}+\mathbb{u}^{1}_{(k,y_h)}\right)\right)_{,y_j}=0 \tag{83}$$

Using (24), the above equation can be re-written as follows

$$\left(L_{ijkh}\ \left(\mathbb{w}^{0}_{(k,x_h)}+\mathbb{w}^{1}_{(k,y_h)}\right)\right)_{,y_j}+\left(L'_{ijkh}\ \left(I_{khmn}+\Psi^{kh}_{mn}\right)\right)_{,y_j}\mathbb{u}^{0}_{(m,x_n)}=0 \tag{84}$$

The solution of (84) for $\mathbb{w}^{1}_{i}(x,y)$ up to a constant is constructed in the form of

$$\mathbb{w}^{1}_{i}(x,y)=c_i^{mn}(y)\ \mathbb{u}^{0}_{(m,x_n)}(x)+\Re_i^{mn}(y)\ \mathbb{w}^{0}_{(m,x_n)}(x) \tag{85}$$

in which $c_i^{mn}(y)$ is the *y*-periodic sensitivity of the characteristic function $\Re_i^{mn}(y)$

$$c_i^{mn}(y)=\frac{\partial\Re_i^{mn}(y)}{\partial P} \tag{86}$$

Inserting (85) into (84) yields

$$\left(L_{ijkh}\ \left(I_{khmn}+\Psi^{kh}_{mn}\right)\right)_{,y_j}\mathbb{w}^{0}_{(m,x_n)}+\left(L_{ijkh}\ \wp^{kh}_{mn}+L'_{ijkh}\ \left(I_{khmn}+\Psi^{kh}_{mn}\right)\right)_{,y_j}\mathbb{u}^{0}_{(m,x_n)}=0 \tag{87}$$

where $\wp_{ij}^{mn}(y)$ is the *y*-periodic sensitivity defined as

$$\wp_{ij}^{kh}(y)=c^{kh}_{(i,y_j)}(y)=\frac{\partial\Psi_{ij}^{kh}(y)}{\partial P} \tag{88}$$

For arbitrary values of $\mathbb{e}_{ij}(w)=\mathbb{w}^{0}_{(i,x_j)}$ and $\mathbb{e}_{ij}(u)=\mathbb{u}^{0}_{(i,x_j)}$, equation (87) yields the following two governing equations on the RVE domain

$$\left(L_{ijkh}(y)\left(I_{khmn}+\Psi^{kh}_{mn}(y)\right)\right)_{,y_j}=0 \tag{89}$$

which is a direct RVE problem, and

$$\left(L_{ijkh}(y)\wp^{kh}_{mn}(y)+L'_{ijkh}(y)\left(I_{khmn}+\Psi^{kh}_{mn}(y)\right)\right)_{,y_j}=0 \tag{90}$$

which is the sensitivity RVE problem.

To solve for the $O(\hat{I}^{0})$ sensitivity equation we integrate the rate form of (73) over the RVE domain which gives

$$\int_{\Theta}\left(L_{ijkh}(y)\ \hat{w}^{1}_{(k,x_h)}\right)_{,y_j}d\Theta+\int_{\Theta}\left(L'_{ijkh}(y)\ \hat{u}^{1}_{(k,x_h)}\right)_{,y_j}d\Theta+\int_{\Theta}L_{ijkh}(y)\left(\hat{w}^{1}_{(k,y_h)}+\hat{w}^{0}_{(k,x_h)}\right)_{,x_j}d\Theta$$
$$+\int_{\Theta}L'_{ijkh}(y)\left(\hat{u}^{1}_{(k,y_h)}+\hat{u}^{0}_{(k,x_h)}\right)_{,x_j}d\Theta=0 \tag{91}$$

The first two terms vanish due to the *y*-periodicity. Consequently, inserting (24) and (85) into (91) yields:

$$\left(\int_{\Theta}\left\{L_{ijkh}(y)\wp^{mn}_{kh}+L'_{ijkh}(y)\left(I_{khmn}+\Psi^{mn}_{kh}\right)\right\}d\Theta\ \hat{u}^{0}_{(m,x_n)}\right)_{,x_j}$$
$$+\left(\int_{\Theta}\left\{L_{ijkh}(y)\left(I_{khmn}+\Psi^{mn}_{kh}\right)\right\}d\Theta\ \hat{w}^{0}_{(m,x_n)}\right)_{,x_j}=0 \tag{92}$$

Let us denote the sensitivity of the macro-stress rate field as

$$\hat{\Sigma}_{ij}=\frac{1}{|\Theta|}\int_{|\Theta|}\hat{\Sigma}_{ij}\ d\Theta=\hat{L}_{ijkh}\ \hat{e}_{kh}(w)+\hat{L}'_{ijkh}\ \hat{e}_{kh}(u) \tag{93}$$

where $\hat{L}'_{ijkh}$ is the sensitivity of the instantaneous macroscopic constitutive tensor given by:

$$\hat{L}'_{ijkh}=\frac{1}{|\Theta|}\int_{\Theta}\left\{L_{ijmn}(y)\wp^{mn}_{kh}+L'_{ijmn}(y)\left(I_{khmn}+\Psi^{mn}_{kh}\right)\right\}d\Theta \tag{94}$$

From (92) one can derive the following macroscopic sensitivity equation:

$$\hat{\Sigma}_{ij,x_j}=0 \tag{95}$$

In summary, the macro-scale sensitivity problem (61)-(65) has the following concise form:

$$\begin{cases}\hat{\Sigma}_{ij,x_j} &= 0 & in & \Omega\\ \hat{\Sigma}_{ij} &= \hat{L}_{ijkh}(\Re)\,\hat{e}_{kh}(w)+\hat{L}'_{ijkh}(\Re,c)\,\hat{e}_{kh}(u) & in & \Omega\\ \hat{e}_{ij}(w) &= \hat{w}^{0}_{(i,x_j)} & in & \Omega\\ w_i &= 0 & on & \Gamma_u\\ \hat{\Sigma}_{ij}n_j &= 0 & on & \Gamma_t\end{cases} \tag{96}$$

### 4.2. *Micro-Scale Sensitivity Problem*

Since the displacement $u_i$ and the characteristic functions $\Re^{kh}_i$ are known prior to the sensitivity analysis (from (35) and (37)), the solution of the boundary value problem (96) is function of $c^{kh}_i$, which can be calculated from the following micro-scale sensitivity problem:

$$\begin{cases} c_i^{mn} & is & y-periodic & & \\ q_{ij,y_j}^{kh} & = & 0 & in & \Theta \\ q_{ij}^{kh} & = & L_{ijmn}(y)c_{(m,y_n)}^{kh} + L'_{ijmn}(y)\,(d_{km}d_{hn} + \Re_{(m,y_n)}^{kh}) & in & \Theta \\ \left[\left|c_i^{mn}\right|\right] & = & 0 & on & g_\Theta \\ \left[\left|q_{ij}^{kh}\,n_j\right|\right] & = & 0 & on & g_\Theta \\ q_{ij}^{kh}\,n_j & is & y-antiperiodic & & \end{cases} \tag{97}$$

where $q_{ij}^{kh}$ is the sensitivity of the stress concentration factors $s_{ij}^{kh}$

$$q_{ij}^{kh} = \frac{\partial s_{ij}^{kh}}{\partial P} \tag{98}$$

The sensitivity $\mathscr{e}_{ij}(w)$ of the local strain rate field is given by:

$$\mathscr{e}_{ij}(w) = \Im_{mn}^{ij}(y)\,\mathscr{e}_{mn}(w) + \wp_{mn}^{ij}(y)\,\mathscr{e}_{mn}(u) \tag{99}$$

The stress rate sensitivity in $\Theta$ is given as

$$\mathscr{S}_{ij} = L_{ijrs}\,\Im_{mn}^{rs}(y)\,\mathscr{e}_{mn}(w) + \left[\,L'_{ijrs}\;\Im_{mn}^{rs}(y) + L_{ijrs}\,\wp_{mn}^{rs}(y)\,\right]\mathscr{e}_{mn}(u) \tag{100}$$

### 4.3. The weak and discrete forms of the sensitivity problem

The weak formulation of the macro-scale sensitivity problem (96) is given as:

$$\begin{cases} find \;\; w_i^0 \in \left[H^1(\Omega)\right]^3 \; such\; that: \\ \\ \displaystyle\int_\Omega \mathscr{S}_{ij}(w)\;\; e_{ij}(j)\,d\Omega = 0; \quad \forall\, j_i \in \left[H^1(\Omega)\right]^3 \end{cases} \tag{101}$$

The discretization of (101) yields the following system of nonlinear equations:

$$R_A = F_A^{ext} - F_A^{\text{int}} = 0 \tag{102}$$

where $R_A$ is the residual vector, and

$$F_A^{\text{int}} = \int_\Omega \mathscr{S}_{kh}\; B_{khA}^{\Omega}\, d\Omega \;\; ; \qquad F_A^{ext} = 0 \tag{103}$$

The nodal components of the displacement sensitivity $W_A^0$ $\left(w_i^0 = N_{iA}^{\Omega} W_A^0\right)$ are obtained using Newton method

$$^{(k+1)}W_A^0 = {}^{(k)}W_A^0 + \Delta W_A^0 \tag{104}$$

$$^{(k)}\mathbb{K}_{AB}\,\Delta W_B^0 = {}^{(k)}R_A - {}^{(k)}\mathbb{K}'_{AB}\,\Delta d_B^0 \tag{105}$$

where $\mathbb{K}_{AB}$ is the macro stiffness matrix for the direct problem (47) and $\mathbb{K}'_{AB}$ the coupling term given by:

$$\mathbb{K}'_{AB} = \int_{\Omega} B_{mnA}^{\Omega}\,\mathbb{L}'_{mnkh}\,B_{khB}^{\Omega}\,d\Omega \tag{106}$$

Note that $\mathbb{L}'_{ijkh}$ is a function of $c_i^{rs}$, which is the solution of the following weak formulation on the microscale:

$$\begin{cases} \quad Find\,(\,c_i^{rs} \in \left[H^1(\Theta)\right]^3\ such\,that: \\ \int_{\Theta} c_{i,j}^{rs}\,L_{ijkh}\,j_{k,h}\,d\Theta = -\int_{\Theta} \Re_{i,j}^{rs}\,L'_{ijkh}\,j_{k,h}\,d\Theta - \int_{\Theta} L'_{ijrs}\,j_{i,j}\,d\Theta\,; \quad \forall\, j_i \in \left[H^1(\Theta)\right]^3 \end{cases} \tag{107}$$

Further discretizing $c_i^{rs} = N_{iA}^{\Theta}\,\aleph_A^{mn}$, the discrete form of (107) yields:

$$\left(\int_{\Theta} B_{khA}^{\Theta}\,L_{khrs}(y)\,B_{khB}^{\Theta}\,d\Theta\right)\aleph_B^{rs} = -\left(\int_{\Theta} B_{khA}^{\Theta}\,L'_{khrs}(y)\,B_{rsB}^{\Theta}\,d\Theta\right)\mathbf{D}_B^{rs} - \int_{\Theta} L'_{khrs}(y)\,B_{khA}^{\Theta}\,d\Theta \tag{108}$$

where $\aleph_A^{mn}$ are the nodal components of the characteristic functions on $\Theta$; Note that the same stiffness matrix is used to solve for the micro-scale direct and sensitivity problems. Procedures for integrating the stress sensitivities are outlined in Section 4.4.

### 4.4 Stress sensitivity update procedure

We start from the rate of stress sensitivity given by

$$\dot{\Sigma}_r = L_r\left(\dot{\varepsilon}_r(w) - \dot{\varepsilon}_r^{\,p}(w)\right) + L'_r\left(\dot{\varepsilon}_r(u) - \dot{\varepsilon}_r^{\,p}(u)\right) \tag{109}$$

where $L'_r$ is the sensitivity of elastic stiffness matrix, which is equal to zero if the sensitivity is not with respect to one of the elastic constants.

The sensitivity of the plastic strain rate, $\dot{\varepsilon}_r^p(w)$, is given as follows:

$$\dot{\varepsilon}_r^p(w) = \dot{l}_r(w)\ \mathrm{N}_r + \dot{l}_r(u)\ \mathrm{N}'_r; \qquad \mathrm{N}'_r = \frac{\partial y_r(\Sigma)}{\partial s_r} \tag{110}$$

where $l_r(w)$ is the sensitivity of the plastic flow parameter. $y_\rho(\Sigma)$ is the sensitivity of the Von Mises yield function at a Gauss point given as

$$y_r(\Sigma) = s_r^{\mathrm{T}}\ P\ \Sigma_r - \frac{2}{3}\hat{s}_r\hat{\Sigma}_r = 0 \tag{111}$$

$\hat{\Sigma}_\rho$ is the sensitivity of the yield stress $s_\rho$:

$$\dot{\hat{\Sigma}}_r = \frac{2}{3}\left(\dot{l}_r(w)\,\mathrm{H}\,\hat{s}_r + \dot{l}_r(u)\,\mathrm{H}'\hat{s}_r + \dot{l}_r(u)\,\mathrm{H}\hat{\Sigma}_r\right) \tag{112}$$

which after the backward Euler integration gives

$${}^{(k+1)}\hat{\Sigma}_r = \left(I + \Delta l_r(u)\,\mathrm{H}\right)^{-1}\left[{}^{(k)}\hat{\Sigma}_r + \frac{2}{3}\left(\Delta l_r(w)\,\mathrm{H}\,{}^{(k+1)}\hat{s}_r + \Delta l_r(w)\,\mathrm{H}'\,{}^{(k+1)}\hat{s}_r\right)\right] \tag{113}$$

where $\mathrm{H}'$ is equal to 1 if the sensitivity parameter is the hardening parameter and zero otherwise. Substituting eqs. (39), (51), (99) and (110) into (109) yields

$$\dot{\Sigma}_r = L_r\left(\Im_r\dot{\varepsilon}_r(w) + \wp_r\dot{\varepsilon}_r(u) - \dot{l}_r(w)\,P\,s_r - \dot{l}_r(u)\,P\,\Sigma_r\right) + L'_r\left(\Im_r\dot{\varepsilon}_r(u) - \dot{l}(u)\,P\,s_r\right) \tag{114}$$

Assuming that ${}^{(k+1)}\wp = {}^{(k)}\wp$ and applying the backward Euler scheme to (114) yields

$${}^{(k+1)}\Sigma_r = \left(I + \Delta l_r(u)\,L_r\,P\right)^{-1}\ \Sigma_r^{trial} \tag{115}$$

where $\Sigma_r^{trial}$ is the trial stress sensitivity given at increment (k+1) by:

$$\Sigma_r^{trial} = {}^{(k)}\Sigma_r + L_r\,{}^{(k)}\Im_r\,\Delta\dot{\varepsilon}(w) + \left(L'_r\,{}^{(k)}\Im_r + L_r\,{}^{(k)}\wp_r\right)\Delta\dot{\varepsilon}(u) - {}^{(k+1)}s_r\,P\left(L'_r\,\Delta l_r(u) + L_r\,\Delta l_r(w)\right) \tag{116}$$

The sensitivity $\Delta l_r(w)$ of the plastic parameter increment is obtained from the Newton method:

$${}^{(k+1)}\Delta l_r(w) = {}^{(k)}\Delta l_r(w) - \left(\frac{\partial y_r}{\partial \Delta l_r(w)}\right)^{-1} y\,\Big|_{{}^{(k)}\Delta l_r(w)} \tag{117}$$

where

$$\frac{\partial y_r}{\partial \Delta l_r(w)} = -{}^{(k+1)}s_r^{\mathrm{T}} P \left( \left( L_r P \right)^{-1} + \Delta l_r(u)\, P \right)^{-1} {}^{(k+1)}s_r - \left( \mathrm{I} + \Delta l_r(u) \mathrm{H} \right)^{-1} \frac{4}{9} \mathrm{H}\, {}^{(k+1)}\hat{s}_r^2 \qquad (118)$$

## 5. Numerical examples

In this section we investigate the accuracy and computational efficiency of the proposed multiscale analytical sensitivity analysis. For simplicity, we consider a composite specimen subjected to uniform tension load. The state of uniform macro-stress is modeled using a single eight-node hexahedral element as shown in Fig. 2.*a*.

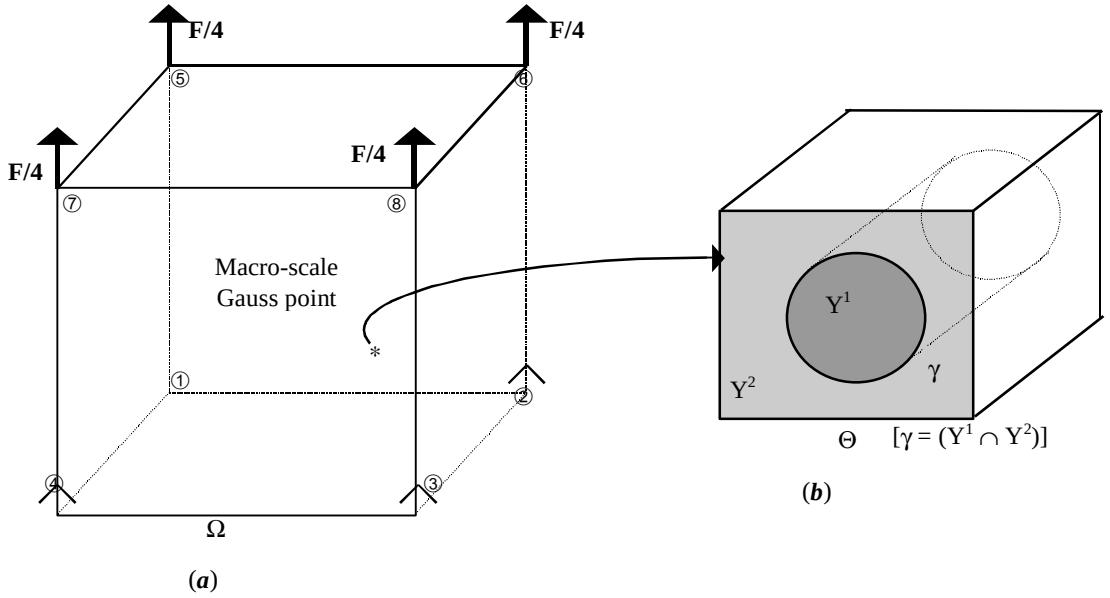


**Figure. 2.** Unidirectional periodic composite: (*a*) macro domain Ω, (b) RVE domain Θ.

Two RVE models have been considered. The first, with isotropic linear elastic micro-constituents. The Multiscale Analytical Sensitivity Analysis (MASA) is performed with respect to the Young's modulus, ***E*,** and Poisson ratio, ***n***. In the second numerical example, we consider an elastic reinforcement embedded in the elasto-plastic matrix. The sensitivity analysis is performed with respect to the hardening parameter, *H*. In both cases, the sensitivity results obtained by the MASA approach are compared to those obtained using CFD method.

### 5.1. Linear elastic composite

The properties of the elastic composite considered are as follows:

*Matrix* (1): Young's Modulus $E_1 = 10^5$ Mpa, Poisson Ratio $\nu_1 = 0.25$.
*Fiber* (2): Young's Modulus $E_2 = 2.10^5$ Mpa, Poisson Ratio $\nu_2 = 0.20$.

In the following we denote $\mathbb{L}^{p_a} = \partial \mathbb{L} / \partial p_a$ and $w^{p_a} = \partial u / \partial p_a$. Tables 1A, 2A, 3A, 4A, give the sensitivity of the macro-constitutive tensor components, $\mathbb{L}_{1111}$, $\mathbb{L}_{3333}$, $\mathbb{L}_{1212}$ and $\mathbb{L}_{2323}$, with respect to the elastic parameters $E_1$, $\nu_1$, $E_2$, $\nu_2$, respectively. The sensitivities obtained by the MASA approach are compared to those computed using CFD method for $d p_a = 1.e^{-2} \times p_a$. The *x*-component $w_1$ ($w_2 = w_1$) and the *z*-component $w_3$ of the displacement sensitivity at node ⑧ are shown in tables 1B, 2B, 3B, 4B, respectively.

Table 1A
Sensitivity of macro constitutive tensor components with respect to $E_1$

| | **MASA** | **CFD** |
|---|---|---|
| $\mathbb{L}^{E_1}_{1111}$ ($e^{-1}$) | 6.091605 | 6.091500 |
| $\mathbb{L}^{E_1}_{3333}$ | 1.038295 | 1.038350 |
| $\mathbb{L}^{E_1}_{1212}$ ($e^{-1}$) | 3.602927 | 3.602950 |
| $\mathbb{L}^{E_1}_{2323}$ ($e^{-1}$) | 2.083333 | 2.083350 |

Table 1B
Sensitivity of the displacement field with respect to $E_1$

| | **MASA** | **CFD** |
|---|---|---|
| $w_1^{E_1}$ ($e^{-9}$) | 4.753287 | 4.755000 |
| $w_3^{E_1}$ ($e^{-8}$) | -4.777277 | -4.77600 |

Table 2A
Sensitivity of macro constitutive tensor components with respect to $E_2$

| | **MASA** | **CFD** |
|---|---|---|
| $\mathbb{L}^{E_2}_{1111}$ ($e^{-1}$) | 5.537794 | 5.538000 |
| $\mathbb{L}^{E_2}_{3333}$ ($e^{-1}$) | 2.403461 | 2.403500 |
| $\mathbb{L}^{E_2}_{1212}$ ($e^{-2}$) | 9.382623 | 9.383000 |
| $\mathbb{L}^{E_2}_{2323}$ ($e^{-1}$) | 2.000000 | 2.000000 |

Table 2B
Sensitivity of the displacement field with respect to $E_2$

| | **MASA** | **CFD** |
|---|---|---|
| $w_1^{E_2}$ ($e^{-9}$) | 5.070172 | 5.065000 |
| $w_3^{E_2}$ ($e^{-8}$) | -1.337427 | -1.338000 |

Table 3A
Sensitivity of macro constitutive tensor components with respect to $\nu_1$

| | **MASA** | **CFD** |
|---|---|---|
| $\mathbb{L}^{\nu_1}_{1111}$ ($e^{+4}$) | 1.019670 | 1.020000 |
| $\mathbb{L}^{\nu_1}_{3333}$ ($e^{+4}$) | 1.297869 | 1.295000 |
| $\mathbb{L}^{\nu_1}_{1212}$ ($e^{+3}$) | -3.002439 | -3.00000 |
| $\mathbb{L}^{\nu_1}_{2323}$ ($e^{+3}$) | -1.736111 | -1.73500 |

Table 3B
Sensitivity of the displacement field with respect to $\nu_1$

| | **MASA** | **CFD** |
|---|---|---|
| $w_1^{\nu_1}$ ($e^{-3}$) | -3.395203 | -3.400000 |
| $w_3^{\nu_1}$ ($e^{-3}$) | -1.317338 | -1.300000 |

Table 4A
Sensitivity of macro constitutive tensor components with respect to $\nu_2$

Table 4B
Sensitivity of the displacement field with respect to $\nu_2$

| | MASA | CFD |
|---|---|---|
| $\hat{L}^{n_2}_{1111}$ ($e^{+4}$) | 1.432844 | 1.43500 |
| $\hat{L}^{n_2}_{3333}$ ($e^{+3}$) | 8.972921 | 8.95000 |
| $\hat{L}^{n_2}_{1212}$ ($e^{+3}$) | -1.501220 | -1.50000 |
| $\hat{L}^{n_2}_{2323}$ ($e^{+3}$) | -3.20000 | -3.20000 |

| | MASA | CFD |
|---|---|---|
| $w_1^{n_2}$ ($e^{-3}$) | -3.186963 | -3.185000 |
| $w_3^{n_2}$ ($e^{-4}$) | 6.179274 | 6.200000 |

In terms of accuracy, the sensitivities obtained by the MASA approach agree well with those computed using CFD approach (0 to 0.4% difference). In terms of computational efficiency, CFD approximation requires two to three factorizations of the elastic macro-stiffness $\hat{K}$ and micro-stiffness $K^{\Theta}$ for each design parameter totaling 16 to 24 factorizations. Using MASA approach, on the other hand, the same sensitivities can be obtained by performing 2 factorizations only.

### 5.2. *Nonlinear elastoplasticity problems.*

The properties of micro-phases considered are as follows:

*Matrix*: Young's Modulus $E_1 = 10^3$ Gpa, Poisson Ratio $\nu_1 = 0.3$, yield stress $s_m = 24$ Mpa, isotropic hardening modulus $H = 2.10^2$ Gpa.
*Fiber*: Young's Modulus $E_2 = 8.10^3$ Gpa, Poisson Ratio $\nu_2 = 0.2$.

The sensitivity analysis is performed with respect to plastic hardening parameter H. Figures 3 and 4 show the evolution of displacement sensitivities, $w_1$ and $w_3$, versus the load parameter, respectively. Results of MASA approach are compared to those of CFD approach for two different values of design parameter step size, $\delta H = 10^{-2}$ H and $\delta H = 10^{-5}$H.

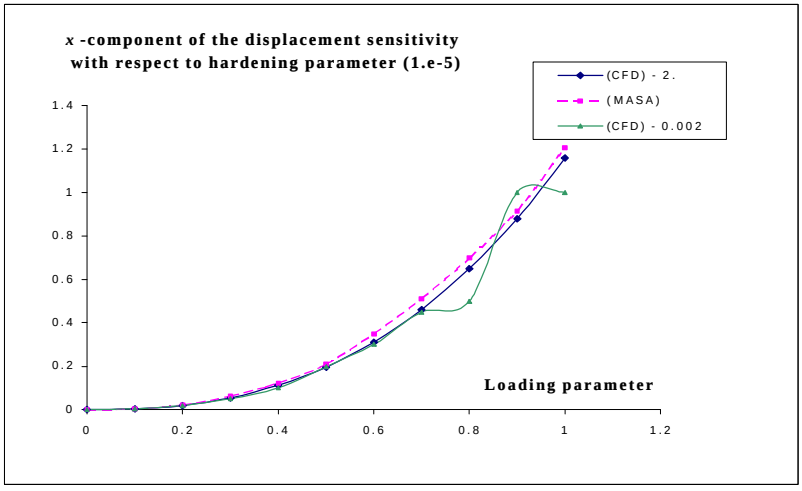


**Figure. 3.** Evolution of *x*-component of the displacement sensitivity versus load parameter for $\frac{H}{E} = \frac{1}{5}$

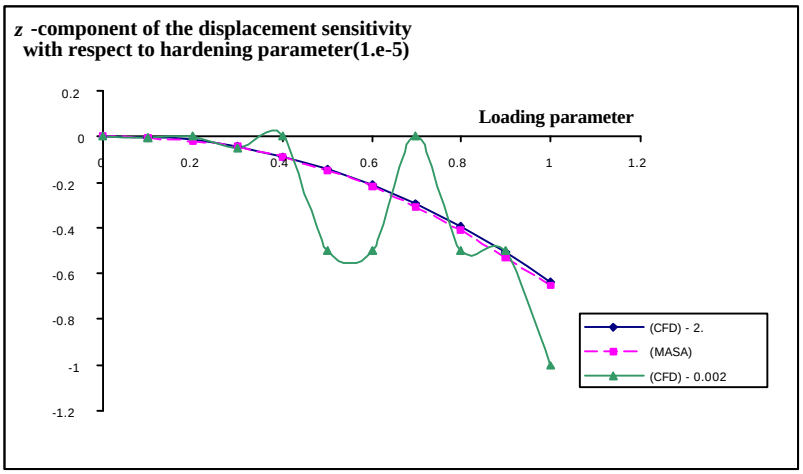


**Figure. 4.** Evolution of *z*-component of the displacement sensitivity versus load parameter for $\frac{H}{E}=\frac{1}{5}$

It can be seen that the sensitivity results obtained by the CFD approximation with the step size, δH = 2., is in good agreement with the MASA approach (0 to 1% relative error). On the other hand, for the value of step size, δH = 0.002, the CFD gives inaccurate resolution of sensitivities. In Figures 4 and 5 we considered the Hardening parameter to Young modulus ratio of $\frac{H}{E}=\frac{1}{5}$. We further study the sensitivities for the Hardening parameter to Young modulus ratio of $\frac{H}{E}=\frac{1}{50}$. The results presented in Figures 5 and 6 show that the optimal value of the step size selected in the previous case results in oscillatory response of the sensitivities. This suggests that the optimal value of the step size in CFD approximation is problem dependent.

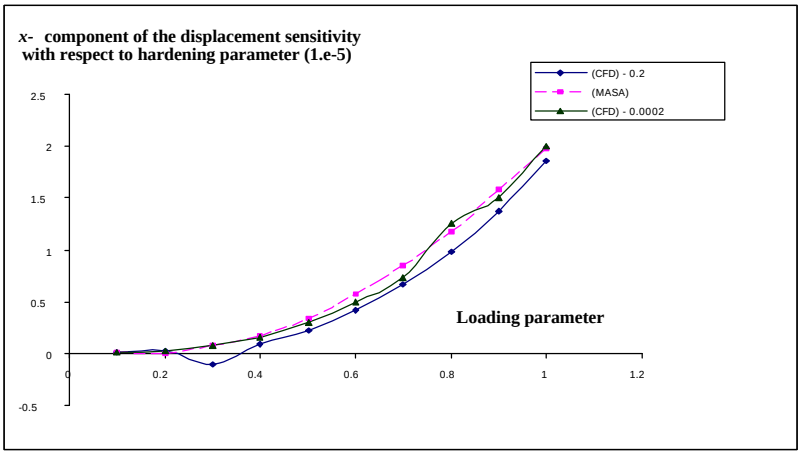


**Figure. 5.** Evolution of the *x*-component of the displacement sensitivity (H = $2.10^1$ Gpa) versus load parameter

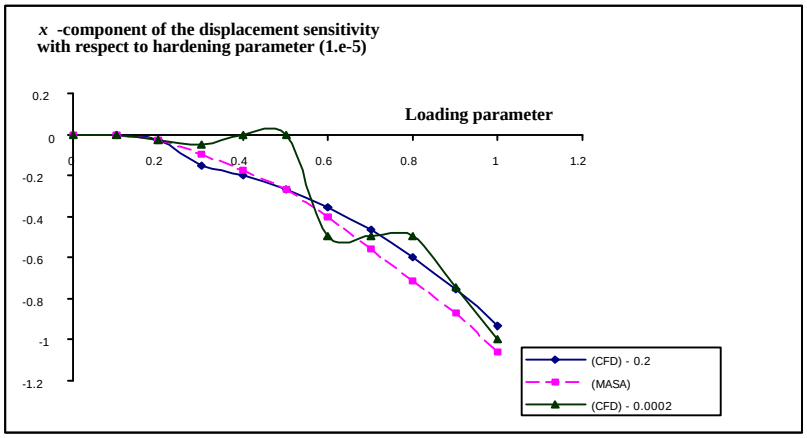


**Figure. 6.** Evolution of the *z*-component of the displacement sensitivity (H = $2.10^1$ Gpa) versus load parameter

## 6. Summary and future research directions

Multiscale analytical sensitivity analysis approach has been developed for inelastic periodic composites. Comparison of the Multiple Scale Sensitivity Analysis to the central finite difference approximation revealed its advantage in terms of accuracy and computation efficiency. We demonstrated that the CFD approximation is highly sensitive to the choice of the step size, whose optimal value is problem dependent.

Despite its significant advantage over the CFD approach, the proposed MASA approach requires significant computational resources for large scale macro-problems with detailed Representative Volume Elements. For nonlinear history dependent problems the RVE problem has to be solved at every increment and for each macroscopic Gauss point. To alleviate this difficulty, in the future work we consider multiple scale sensitivity analysis in the context of mathematical homogenization theory with eigenstrains [22], [23]. By this approach, the history data is updated only at two or three points within a microstructure, i.e., one for each phase.

## 7. Acknowledgment

The support of the Office of Naval Research through grant number N00014-97-1-0687 is gratefully acknowledged.

## 8. References

[1] J. M. Guedes and Kikuchi, Preprocessing and Postprocessing for materials based on the homogenization method with adaptive finite element methods, Comput. Methods Appl. Mech. Engrg. 83, 1990.
[2] N. Kikuchi, S. Nishiwaki, J. S. Ono Fonseca and E. C. Nelli Silva, Design optimization method for compliant mechanisms and material microstructure, Comput. Methods Appl. Mech. Engrg. 151, 1998.
[3] M. A. Ghouali and G. Duvaut, Local Analytical Sensitivity Analysis (LASA) for shape optimization of unidirectional composites, ICCE/5 International Conference on Composites Engineering, Las-Vegas, 1998.
[4] G. Duvaut and G. Terrel, Optimization of fiber-reinforced composites, Second International Conference on Composite Science and Technology, Durban, South-Africa, 1999.
[5] R.T. Haftka and R. V. Grandhi, Structural shape optimization - A survey, Comput. Methods Appl. Mech. Engrg. 57, 1986.

[6] R.T. Haftka, Z. Gürdal and M. P. Kamat, Element of structural optimization, Kluwer Academic Publishers (1990).
[7] U. Kirsh, Structural optimization, Fundamentals and applications, Springer-Verlag, 1993.
[8] H. S. Kohli and G. F. Carey, Shape optimization using adaptive shape refinement, Internat. J. Numer. Methods Eng., Vol 36, $N^0$ 14, 2435-2452 (1993).
[9] J. S. Arora and J. E. B. Cardoso, A variationnal principle for shape design sensitivity analysis, AIAA J. 30 (5) (1992).
[10] D. A. Tortorelli and R. B. Haber, First-order design sensitivity analysis for rate-independent elastoplasticity, Compt. Meths. Appl. Mech. Engrg. 107, (1993).
[11] M. A. Ghouali, G. Duvaut, S. Ortola and A; Oster, Local analytical design sensitivity analysis of the forging problem using FEM, Compt. Methods Appl. Mech. Engrg. 172 (1999).
[12]-S. Kibsgaard, Sensitivity analysis - the basis for the optimization, Internat. J. Numer. Methods Eng., Vol 34, 901-932 (1992).
[13] C. A. Vidal and R. B. Haber, Design sensitivity analysis for rate-independent elastoplasticity, Comput. Methods Appl. Mech. Eng., Vol 107, (1993).
[14] E. J. Haug and J. S. Arora, Design sensitivity analysis of elastic mechanical systems, Compt. Meths. Appl. Mech. Engrg. 15, (1978).
[15] O. Pironneau, Optimal shape design for elliptic systems, Springer-Verlag, 1984
[16] E. J. Haug, K. K. Choi and V. Komkov, Design sensitivity analysis in structural systems. Academic Press, New York, 1986.
[17] J. Sokolowski and J.P. Zolesio, Introduction to shape optimization. Shape sensitivity analysis, Springer-Verlag, 1992.
[18] M. A. Ghouali, Local analytical sensitivity analysis for shape optimization, CSME Forum, Symposium on the Mechanics of Solids and Structures materials technology, Vol 3, Toronto, 1998.
[19] D. Post, Moire Interferometry, Chap. 7, Handbook of Experimental Mechanics, A. S. Kobayashi, Editor, Prentice-Hall, Englewood Cliffs, NJ, (1987).
[20] D. Post and J. D. Wood, Determination of thermal strains by moire interferometry, Experimental Mechanics, 29(3), (1989).
[21] D. G. Phelan et R. B. Haber, Sensitivity analysis of linear elastic domain using domain parametrization and a mixed mutual energy principles. Comput. Methods Appl. Mech. Engrg., Vol 77, 1989.
[22] J. Fish, K. Shek, M. Pandhereradi and M. S. Shephard, Computational Plasticity for Composite Structures Based on Mathematical Homogenization: Theory and Practise, Comput. Methods Appl. Mech. Engrg. 148, 1997.
[23] J. Fish and K. Shek, Finite Deformation Plasticity for Composite Structures: Computational Models and Adaptive Strategies, Comput. Methods Appl Mech. Engrg, Vol 172, 1999.
[24] K. Terada and N. Kikuchi, Microstructural Design of Composites Using the Homogenization Method and Digital Images, Materials Science Research International, Vol.2-No. 2, 1996, pp.65-72.